Synthesis, protonation and Cu^{2+} co-ordination studies on a new family of thiophenophane receptors †

Juan A. Aguilar,[a] Pilar Díaz,[b] Antonio Doménech,[c] Enrique García-España,[b] José M. Llinares,[a] Santiago V. Luis,[d] José A. Ramírez[b] and Conxa Soriano[a]

[a] *Departamento de Química Orgánica, Facultad de Farmacia, Universidad de Valencia, 46100 Burjassot, Valencia, Spain*
[b] *Departamento de Química Inorgánica, Universidad de Valencia, C/ Dr. Moliner 50, 46100 Burjassot, Valencia, Spain*
[c] *Departamento de Química Analítica, Universidad de Valencia, C/ Dr. Moliner 50, 46100 Burjassot, Valencia, Spain*
[d] *Departamento de Química Inorgánica y Orgánica, Universidad Jaume I, Carretera Borriol s/n, 12080 Castellón, Spain*

Received (in Cambridge) 26th January 1999, Accepted 12th April 1999

The synthesis of the new thiophenophanes 2,5,8,11-tetraaza[12](2,5)thiophenophane (L^1), 2,6,9,13-tetraaza-[14](2,5)thiophenophane (L^2) and 2,5,8,11,14-pentaaza[15](2,5)thiophenophane (L^3) is described. The stepwise protonation constants of the macrocycles are determined by pH-metric titration and their protonation patterns are analysed by means of ^1H and ^{13}C NMR spectroscopy. L^1 and L^2 present first protonation on the thenylic nitrogens while L^3 protonates first on the central nitrogens of the polyamine bridge. Molecular orbital calculations are used to locate the atomic orbitals contributing to the HOMO of the free amines. The interaction with Cu^{2+} shows for L^1 and L^3 formation of binuclear complexes which readily hydrolyse to give very stable species. Electrochemical studies show for all three Cu^{2+}–receptor systems an important stabilisation of the Cu^+ oxidation state towards its disproportionation into Cu^{2+} and Cu^0 oxidation states.

In recent years we have been investigating the chemistry of a series of cyclophanes characterised by the presence of single or condensed aromatic spacers interrupting polyamine chains with different numbers of nitrogen donors and a variety of hydrocarbon chains between them. The acid–base properties and co-ordination chemistry of these ligands were strongly affected by the type of spacer introduced as well as by the length and number of nitrogen atoms in the polyamine bridge.[1–10]

For instance, and contrary to expectations, NMR and microcalorimetric studies proved that the benzylic nitrogens were the first sites bearing protonation in the tri- or tetraaza macrocycles containing either 1,4-benzene or 1,4-durene ‡ spacers. Moreover, the tetraazaparacyclophane 2,5,8,11-tetraaza[12]paracyclophane (L^4) was, as far as we know, one of the first tetraaza-macrocycles containing a continuous set of nitrogen donors linked by ethylenic chains able to co-ordinate two metal ions[7] and, even more, formation of tetranuclear Cu^{2+} complexes was observed when substituting the 1,4-benzene spacer in L^4 for a 1,4-naphthalene moiety (L^{10}). In the latter case, each macrocycle co-ordinated two Cu^{2+} ions being the metal ions of the two different subunits interconnected by μ-hydroxo bridges.[8]

A further step in the development of this research was the introduction of spacers themselves containing additional heteroatoms. Here we present the synthesis and acid–base behaviour of the thiophenophane ligands 2,5,8,11-tetraaza-[12](2,5)thiophenophane (L^1), 2,6,9,13-tetraaza[14](2,5)thiophenophane (L^2) and 2,5,8,11,14-pentaaza[15](2,5)thiophenophane (L^3). Additionally, in order to better understand the protonation patterns of these compounds, we have performed preliminary molecular orbital calculations to localise the frontier orbitals in the free amines. Finally, the Cu^{2+} co-ordination characteristics of the three receptors have been examined from both thermodynamic and electrochemical points of view. Since related receptors containing 1,4-benzene or 1,4-durene spacers yielded significant stabilisation of the Cu^+ oxidation towards disproportionation,[9,10] special interest has been devoted to this aspect.

Experimental

Synthesis of the ligands

2,5-Bis(bromomethyl)thiophene. 2,5-Bis(bromomethyl)thiophene was obtained by reacting 2,5-dimethylthiophene and *N*-bromosuccinimide in CCl_4. The reaction was induced with visible light. The resulting mixture was filtered and the solution evaporated to dryness. The solid residue was recrystallised from hexane, yield 69%. ^1H NMR δ_H ($CDCl_3$), 4.66 (s, 4H), 6.93 (s, 2H).

2,5,8,11-Tetrakis(*p*-tolylsulfonyl)-2,5,8,11-tetraaza[12](2,5)-thiophenophane. 1,4,7,10-Tetrakis(*p*-tolylsulfonyl)-1,4,7,10-tetraazadecane (6.4 g, 7.4 mmol)[1] and K_2CO_3 (24 mmol) were suspended in refluxing CH_3CN (300 cm^3). To the mixture was added dropwise a freshly prepared solution of 2,5-bis(bromomethyl)thiophene in CH_3CN (100 cm^3). After the addition was completed, the suspension was refluxed for 24 h, then filtered and the solution evaporated to dryness. The solid product was recrystallised from dichloromethane–hexane, yield 64%, mp 195–198 °C; ^1H NMR δ_H ($CDCl_3$), 2.46 (s, 12H), 2.75 (s, 4H),

† Figure S1 (Plots of ^1H–^1H and ^1H–^{13}C correlated NMR spectra of triprotonated L^3 at pH = 4.5 recorded in D_2O at room temperature) and Figure S2 (Plots of the ^{13}C NMR chemical shifts of the aliphatic carbon atoms as a function of pH. A) L^1, B) L^2 and C) L^3) are available as supplementary data. For direct electronic access see http://www.rsc.org/suppdata/p2/1999/1159, otherwise available from BLDSC (SUPPL. NO. 57539, pp. 4) or the RSC Library. See Instructions for Authors, available *via* the RSC web page (http:www.rsc.org/authors).
‡ Durene = 1,2,4,5-tetramethylbenzene.

2.97–3.05 (m, 4H), 3.06–4.01 (m, 4H), 4.26 (s, 4H), 6.85 (s, 2H), 7.33 (d, J = 8 Hz, 4H), 7.38 (d, J = 8 Hz, 4H), 7.70 (d, J = 8 Hz, 4H), 7.75 (d, J = 8 Hz, 4H); ^{13}C NMR δ_C ($CDCl_3$), 21.2(2), 47.0, 48.1, 49.0, 50.0, 127.0, 127.3, 128.1, 129.6, 129.7, 133.0, 135.0, 138.8, 143.5, 143.9; MS *m*/*z* (FAB) 873 $(M + 2H)^+$.

2,5,8,11-Tetraaza[12](2,5)thiophenophane (L^1). 2,5,8,11-Tetrakis(*p*-tolylsulfonyl)-2,5,8,11-tetraaza[12](2,5)thiophenophane (2 g, 2.3 mmol), NaH_2PO_4 (5 g, 35 mmol) and 4% sodium amalgam (50 g) were suspended in a mixture of MeOH–THF (5 cm^3 : 100 cm^3) and refluxed for 72 h. The suspension was filtered, and the organic solvents evaporated. To the residue was added water (5 cm^3) and this was then extracted with CH_2Cl_2. After vacuum evaporation, the oily product was chromatographed on silica (MeOH–NH_3) to give the pure product. The hydrobromide salt was finally obtained by adding aqueous HBr to an ethanolic solution of the free amine, yield 46%, mp 215–216 °C; ^{1}H NMR δ_H (D_2O), 3.00 (s, 4H), 3.02 (t, J = 7 Hz, 4H), 3.29 (t, J = 7 Hz, 4H), 4.53 (s, 4H), 7.31 (s, 2H); ^{13}C NMR δ_C (D_2O), 42.1, 43.5, 43.6, 45.9, 134.9, 135.2. Anal. Calc. for $C_{12}H_{26}Br_4N_4S$: C, 25.1; H, 4.5; N, 9.8. Found: C, 25.1; H, 4.6; N, 9.8%.

2,6,9,13-Tetrakis(*p*-tolylsulfonyl)-2,6,9,13-tetraaza[14](2,5)-thiophenophane. Yield, 90%, mp 191–194 °C; ^{1}H NMR δ_H ($CDCl_3$), 1.63–1.65 (m, 4H), 2.40 (s, 6H), 2.42 (s, 6H), 2.84 (s, 4H), 3.01–3.07 (m, 8H), 4.25 (s, 4H), 6.79 (s, 2H), 7.24–7.34 (m, 8H), 7.61–7.70 (m, 8H); ^{13}C NMR δ_C ($CDCl_3$), 21.5(2), 29.4, 47.8, 47.9, 48.0, 49.7, 127.1, 127.2, 127.3, 129.7, 129.9, 135.0, 135.1, 140.8, 143.5, 143.8; MS *m*/*z* (FAB) 899 $(M - H)^+$.

2,6,9,13-Tetraaza[14](2,5)thiophenophane (L^2). Obtained as its tetrahydrobromide salt. Yield, 46%. ^{1}H NMR δ_H (D_2O), 1.86–1.96 (m, 4H), 3.02 (t, J = 4 Hz, 4H), 3.07 (t, J = 6 Hz, 4H), 3.18 (s, 4H), 4.40 (s, 4H), 7.15 (s, 2H); ^{13}C NMR δ_C (D_2O), 22.8, 42.5, 43.7, 44.9, 45.2, 133.9, 134.5. Anal. Calc. for $C_{14}H_{30}Br_4N_4S$: C, 27.7; H, 5.0; N, 9.2. Found: C, 28.1; H, 5.2; N, 8.9%.

2,5,8,11,14-Pentakis(*p*-tolylsulfonyl)-2,5,8,11,14-pentaaza-[15](2,5)thiophenophane. Yield 66%, mp 260–265 °C; ^{1}H NMR δ_H ($CDCl_3$), 2.33 (s, 3H), 2.34 (s, 6H), 2.35 (s, 6H), 3.03–3.04 (m, 16H), 4.27 (s, 4H), 6.64 (s, 2H), 7.21 (d, J = 8 Hz, 4H), 7.26 (d, J = 8 Hz, 6H), 7.51 (d, J = 8 Hz, 2H), 7.61 (d, J = 8 Hz, 4H), 7.64 (d, J = 8 Hz, 4H); ^{13}C NMR δ_C ($CDCl_3$), 21.6(3), 46.3, 48.4, 50.5(2), 51.4, 127.5, 127.6, 127.7, 128.4, 130.0(2), 133.7, 134.7, 135, 139.0, 144.0, 144.1; MS *m*/*z* (FAB) 1068 $(M - H)^+$.

2,5,8,11,14-Pentaaza[15](2,5)thiophenophane (L^3). Obtained as its pentahydrobromide salt. Yield 44%, mp 235–240 °C; ^{1}H NMR δ_H (D_2O), 3.04 (t, J = 6 Hz, 4H), 3.12 (t, J = 6 Hz, 4H), 3.29 (s, 8H), 4.52 (s, 4H), 7.24 (s, 2H); ^{13}C NMR δ_C (D_2O), 42.5, 43.8, 44.9, 45.8, 46.0, 134.3, 134.7. Anal. Calc. for $C_{14}H_{32}Br_5N_5S$: C, 23.9; H, 4.6; N, 10.0. Found: C, 24.0; H, 4.67; N, 10.0%.

Emf measurements

The potentiometric titrations were carried out in 0.15 mol dm^{-3} $NaClO_4$ or 0.15 mol dm^{-3} NaCl at 298.1 ± 0.1 K, by using the experimental procedure (burette, potentiometer, cell, stirrer, microcomputer, *etc*.) that has been fully described elsewhere.[11] The acquisition of the emf data was performed with the computer program PASAT.[12] The reference electrode was an Ag/AgCl electrode in saturated KCl solution. The glass electrode was calibrated as a hydrogen-ion concentration probe by titration of known amounts of HCl with CO_2-free NaOH solutions and determining the equivalent point by the Gran's method,[13] which gives the standard potential, $E°$, and the ionic product of water (pK_w = 13.73(1)). The concentrations of Cu^{2+} solutions were determined gravimetrically by standard methods.

The computer program SUPERQUAD,[14] was used to calculate the protonation and stability constants. The DISPO[15] program was used to obtain the distribution diagrams. The titration curves for each system (*ca.* 150 experimental points corresponding to at least three measurements, pH range investigated 2–10.5, concentration of ligands was 2×10^{-3} mol dm^{-3} and that of Cu^{2+} was in the range 1×10^{-3}–4×10^{-3} mol dm^{-3}) were treated either as a single set or as separated curves without significant variations in the values of the stability constants. Finally, the sets of data were merged together and treated simultaneously to give the final stability constants.

Spectroscopy

The ^{1}H and ^{13}C NMR spectra were recorded on Varian UNITY 300 and UNITY 400 spectrometers, operating at 299.95 and 399.95 MHz for ^{1}H and at 75.43 and 100.58 MHz for ^{13}C respectively. The spectra of compounds L^1–L^3 were obtained at room temperature in D_2O or DMSO solutions. For the ^{13}C NMR spectra dioxane was used as a reference standard (δ_C = 67.4 ppm) and for the ^{1}H spectra the solvent signal. The pH was calculated from the measured pD values using the correlation, pH = pD − 0.4.[16]

Electrochemistry

Cyclic voltammograms were obtained using the three-electrode arrangement already described.[9] Hanging mercury drop electrode and glassy carbon were used as the working electrodes. A saturated calomel reference electrode (SCE) was used as a reference electrode. Differential pulse voltammetric experiments were performed with a Metrohm E506 Polarecord stand. The potential scan rate was 1–10 mV s^{-1}. Electrochemical experiments were performed in solutions of $Cu(NO_3)_2 \cdot 3H_2O$ or $Cu(ClO_4)_2 \cdot 2H_2O$ (Merck) in doubly distilled water. Ligands were prepared and purified as already described. $NaClO_4$ 0.15 mol dm^{-3} was used as supporting electrolyte. The pH was adjusted to the required value by adding the appropriate amounts of $HClO_4$ and/or NaOH.

Extended Hückel molecular orbital calculations

All calculations were performed by using a package of programs for molecular orbital analysis by Mealli,[17] based on CDNT (atom Cartesian co-ordinate calculations), ICON (extended Hückel method with the weighted H_{ij} formula) and FMO (fragment molecular orbital) including the drawing program CACAO (computer-aided composition of atomic orbitals). The optimisation of the molecular conformations was performed by using the program HYPERCHEM.[18]

Results and discussion

Synthesis

The synthesis of the thiophenophanes L^1–L^3 was carried out by a modification of the general Richman and Atkins procedure employed for the preparation of azamacrocycles.[19] This method, which we had previously used for the synthesis of the related azaparacyclophanes L^4–L^6,[1] consists of the reaction of the corresponding tosylated polyamine with 2,5-bis(bromomethyl)thiophene in refluxing CH_3CN using K_2CO_3 as the base. It is to be noted that high dilution conditions are not required to obtain the cyclised products in high yields (64–90%). 2,5-Bis(bromomethyl)thiophene was generated *in situ* by reaction of *N*-bromosuccinimide and 2,5-dimethylthiophene, being induced by visible light. Detosylation of the cyclic amine was best carried out with a Na/Hg amalgam in buffered methanolic solution.[20] When necessary purification was performed by silica gel chromatography with MeOH–NH_3 as the eluent.[1]

Table 1 Logarithms of the stepwise protonation constants of the cyclophanes L^1–L^3 determined in 0.15 mol dm^{-3} NaCl at 298.1 K. The stepwise protonation constants of the cyclophanes L^4–L^6 and those of the dibenzylated open-chain polyamines L^7–L^9 are also included for comparison

Reaction	L^{1a}	L^{2a}	L^{3a}	L^{4b}	L^{5b}	L^{6b}	L^{7c}	L^{8c}	L^{9c}
$L + H \leftrightarrow HL$ [d]	9.37(1)[e]	10.22(2)	10.36(3)	9.39	9.93	10.68	9.30	9.68	9.85
$HL + H \leftrightarrow H_2L$	8.35(2)	8.90(3)	9.18(2)	8.45	9.09	9.29	8.62	8.87	8.89
$H_2L + H \leftrightarrow H_3L$	5.04(2)	7.39(4)	8.02(3)	5.38	7.44	8.66	6.41	7.37	7.99
$H_3L + H \leftrightarrow H_4L$	2.69(4)	4.20(6)	4.16(4)	2.51	3.61	7.23	3.77	4.90	4.93
$H_4L + H \leftrightarrow H_5L$						3.93			2.75

[a] This work. [b] Taken from ref. 6, 0.15 mol dm^{-3} $NaClO_4$, 298.1 K. [c] Taken from ref. 6, 0.15 mol dm^{-3} $NaClO_4$, 298.1 K. [d] Charges have been omitted for clarity. [e] Numbers in parentheses are standard deviations of the last significant figure.

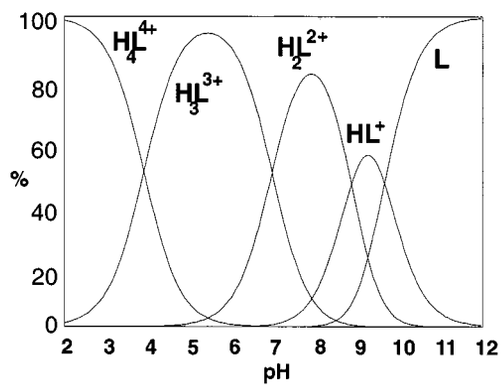

Fig. 1 Distribution for the species existing in equilibria in the system H^+–L^3.

Acid–base behaviour

In Table 1 are presented the logarithms of the basicity constants of the thiophenophanes L^1-L^3 together with those we have previously reported for the related azaparacyclophanes L^4–L^6 and those for the non-cyclic dibenzylated polyamines L^7–L^9.[21,22] In Fig. 1 is plotted the distribution diagram for L^3.

L^1 displays a group of two relatively high constants (log $K_{HL} = 9.37(1)$, log $K_{H_2L} = 8.35(2)$), an intermediate one (log $K_{H_3L} = 5.04(2)$) and a much lower constant for the last protonation step (log $K_{H_4L} = 2.69(4)$). L^2, with a symmetric set of two propylenic chains and one central ethylenic chain, presents relatively high basicity in its three first protonation steps and much reduced basicity in its last protonation step (Table 1).

All this grouping of constants can be explained by considering the electrostatic repulsion between charged ammonium groups to be the major factor affecting the successive protonation steps. For instance, in the case of L^1, while both the first two protonations may occur on non-adjacent nitrogen atoms, the third one should take place on a nitrogen atom adjacent to one already protonated nitrogen and the last one on a nitrogen next to two already protonated nitrogens producing, therefore, a drastic reduction in the basicity constant. Similar considerations would explain the sequence of protonation constants found for L^2 although, in this case, the presence of the larger propylenic chains yields more moderate reductions in basicity in the different steps. As a matter of fact, the constant found for the last protonation of L^2 (log $K_{H_4L} = 4.20(6)$), which has to occur on a nitrogen atom separated from the adjacent ammonium groups by an ethylenic and a propylenic chain, is clearly higher than the corresponding one for L^1 (log $K_{H_4L} = 2.69(4)$).

These basicity trends parallel the behaviour displayed by the related cyclophanes L^4 and L^5 as is reflected by the similar basicity constants found for both types of macrocycles (Table 1).[21]

The effects of the cyclic topology on basicity can be analysed by comparing the basicities of the different cyclophane families with those of their dibenzylated open-chain counterparts. A larger charge accumulation due to the cyclic topology is only observed for the smallest thiophenophane L^1 containing just ethylenic chains, which displays significant lower overall basicity (log $\beta_{H_4L} = 25.5$) than its related open-chain counterpart L^7 (log $\beta_{H_4L} = 28.1$). However, L^2 presents almost the same overall basicity as L^8 (log $\beta_{H_4L} = 30.7$ and 30.8, respectively). A similar behaviour was again observed for azaparacyclophanes L^4 and L^5.

Significant differences are found for the next terms of both series of cyclic receptors, L^3 and L^6 (see Scheme 1). While both receptors present large basicities in their three first protonation steps, L^3 shows a much reduced constant for its fourth protonation step. Moreover, for L^3 just four out of the five possible protonation constants were measurable in the pH range available for the potentiometric studies (pH 2.0–11.0). On the other hand, although L^3 and L^9 present similar basicities in their three first protonation steps, the constant for the fourth protonation step is significantly lower for L^3, which can probably be attributed to a higher charge accumulation at this stage in the cyclic ligand.

In order to get further insight into the protonation patterns of these compounds we have studied the variations of their ^1H and ^{13}C NMR chemical shifts with pH. The ^1H NMR spectrum of L^1 at pH 12.0, where the non-protonated free amine predominates, consists of singlet signals at 3.78 and 2.28 ppm (protons H1 and H4, respectively; for the numbering see Scheme 1) and of two triplet signals at 2.57 and 2.35 ppm (protons H2 and H3, respectively). The aromatic protons (HT2) appear at this pH as a singlet signal at 6.80 ppm. The ^{13}C NMR spectrum consists at the same pH of six signals at 46.27, 47.49, 47.76, 48.43, 128.28 and 144.32 ppm that can be attributed to carbon atoms C2, C4, C1, C3, CT2 and CT1 respectively. The number of ^1H and ^{13}C signals remains constant throughout the whole of the studied pH range indicating that the two-fold symmetry presented by these ligands is preserved upon protonation of the free amines. Similar spectral characteristics are displayed by L^2 and L^3 which both present seven ^{13}C NMR signals. Nevertheless, the protonation of the nitrogens produces significant changes in the ^1H spin-systems that will be discussed below.

All the assignments have been made on the basis of two-dimensional ^1H–^1H and ^1H–^{13}C correlations as well as taking into account the data in the bibliography for similar systems. It is to be noted that, for these compounds, the ^{13}C chemical shifts of the thenylic (thenyl = thienylmethyl) carbon atoms show a very important upfield shift with respect to the analogue benzylic carbons of the benzene counterparts; their chemical shifts being similar to those observed for the methylenic carbons of the ethylenic chains.

As is well known, upon protonation the signals of the protons placed α and of the carbon atoms placed β to the nitrogen atoms bearing protonation are the ones shifting most.[23,24] In fact, in this kind of compound the variations with pH of the chemical shifts of the quaternary carbon atoms of the aromatic rings are particularly useful to establish their average protonation patterns, since they are only in the β-position with respect to nitrogen atoms labelled N1 (Scheme 1).[6,21,22] In Fig. 2 such variations are plotted for all three ligands. For L^1 the largest upfield shifts are produced on going from pH 10 to 5 and for L^2 from pH 10 to 7, suggesting that for both ligands the first two

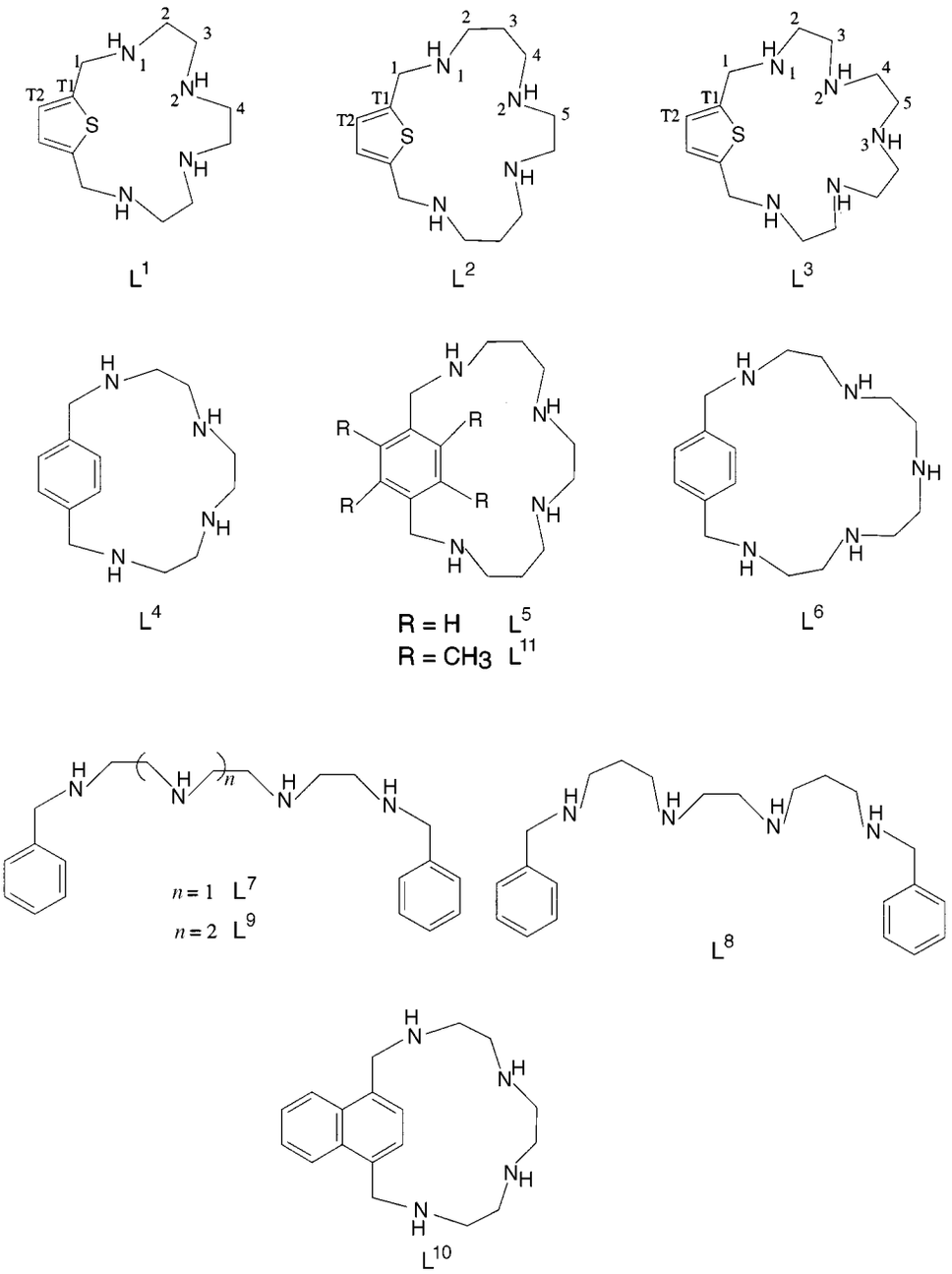

Scheme 1

protonations are mainly affecting the thenylic nitrogen atoms (see Scheme 2). In L^1, this is further confirmed by the upfield shift experienced over the same pH range by the signal of carbon C3, also in a position β to N1, and by the signals of carbons C2 and C4, both β to the central nitrogen of the polyamine chain (N2) which only shift significantly upfield below pH 5, when the third proton binds to L^1 (see supplementary Figure S2).† Similarly, for L^2 the signal assigned to C5, β to N2, only moves upfield below pH 7, again corresponding to the third protonation. The signal of the central carbon of the propylenic chain (C3) continuously shifts upfield throughout all the pH range in agreement with its location β with respect to all nitrogen atoms of L^2. All these data lead us to infer the average protonation mechanism proposed in Scheme 2.

The situation for L^3 is however somewhat different. In Fig. 2C it can be seen that, in this case, the signal of the carbon atom (CT1) just moves upfield on going from pH 8 to 6 which, as shown in the distribution diagram (see Fig. 1), corresponds to the pH range when the third protonation takes place. Therefore, both of the first two protonations should occur in the central part of the polyamine chain (N2 and N3). The signal of C5 shifts upfield from pH 12 to 7.5, remains almost steady from pH 7.5 to 4.5 and again moves upfield below pH 4.5 when the fourth protonation occurs (see Fig. 3). The third protonation causes an important downfield shift of the signal C2, probably suggesting that at this stage a reorganisation of the molecule is produced in such a way that a minimum electrostatic repulsion situation is achieved. This would imply the location of the three protons on non-adjacent nitrogens throughout the molecule with the consequent change in the initial position of the two first protons (see Scheme 2).

The ^{1}H NMR spectra of L^3 recorded at different pH values also reflect this situation (Fig. 3). In this sense, the changes that protonation produces in the spin-systems of the protons of the ethylenic chains somehow reveal the actual protonation state of the compounds. At pH 12, where the free amine predominates, the proton signals of the two ethylenic chains present A4 spin-systems. The first protonation yields a change in the spin-system from A4 to AA′BB′ of the protons of the ethylenic chains defined by carbon atoms C4–C5. This lower equivalence

Table 2 Logarithms of the formation constants of the Cu^{2+} complexes of the receptors L^1–L^3, determined in 0.15 mol dm^{-3} NaCl at 298.1 K. Stability constants for the copper(II) complexes of paraazacyclophanes L^4–L^6 are also included

Reaction[a]	L^1	L^2	L^3	L^{4c}	L^{5c}	L^6
$Cu + L = CuL$	11.89(3)[b]	12.39(2)	14.46(4)	10.41	13.02	17.73
$Cu + L + H = CuHL$	18.48(1)	20.13(5)	21.86(6)	16.92	20.82	26.86
$Cu + L + 2H = CuH_2L$	22.24(3)	26.62(4)	27.25(8)	—	—	33.28
$Cu + L + H_2O = CuL(OH) + H$	3.14(4)	3.26(5)	—	2.27	3.92	—
$CuL + H = CuHL$	6.59	7.74	7.4	6.51	7.80	9.13
$CuHL + H = CuH_2L$	3.76	6.49	5.39			
$CuL + H_2O = CuL(OH) + H$	−8.75	−9.13		−8.14	−9.10	−11.08
$2Cu + L = Cu_2L$	—	—	19.23(6)	—	—	24.29
$2Cu + L + H_2O = Cu_2L(OH) + H$	10.26(2)	—	12.54(5)	—	—	16.95
$2Cu + L + 2H_2O = Cu_2L(OH)_2 + 2H$	3.76(2)	—	2.45(8)	3.44	—	7.50
$2Cu + L + 3H_2O = Cu_2L(OH)_3 + 3H$	−6.58(3)	—	—	—	—	—
$CuL + Cu = Cu_2L$			4.8			6.56
$Cu_2L + H_2O = Cu_2L(OH) + H$			−6.7			−7.34
$Cu_2L(OH) + H_2O = Cu_2L(OH)_2 + H$	−6.5		−9.89			−9.45

[a] Charges omitted for clarity. [b] Numbers in parentheses are standard deviations of the last significant figure. [c] Constants taken from references 4 and 7 and written without standard deviations.

of the protons is due to protonation of N2. Between pH 7.5 and 4.5 both different ethylenic chains display an AA′BB′ spin-system in agreement with the proposed alternate disposition of charged nitrogens in the macrocycle. At lower pH, the observed spin-systems reflect the greater equivalence of the chemical environment of the molecule and protons of carbons C4 and C5 recover the A4 pattern already observed in the pH values range where all nitrogens were non-protonated.

The protonation behaviours observed for these compounds correspond quite closely to those displayed by their related azaparacyclophanes and dibenzylated open-chain polyamines. Namely, L^1 behaves similarly to L^4 and L^7 while L^2 presents an analogous protonation pattern to those of L^5 and L^8. On the other hand, at least in its first protonation steps, L^3 resembles L^6 and L^9.

Whether the thenylic or benzylic nitrogens protonate in the first place or not should depend on the local electron densities of the different nitrogens as well as on solvation effects. Since an acid–base process implies electron sharing between the HOMO of the base and the LUMO of the acid, identifying the location of the HOMO of the base could help in understanding the discussed protonation behaviours. Protonation would be favoured on the nitrogen atoms whose atomic orbitals contribute to the HOMO. Indeed, molecular orbital calculations performed with the program CACAO[17] show the participation of atomic orbitals from the aromatic ring and from the thenylic or benzylic nitrogens in the HOMO of the free amines L^1, L^2, L^4 and L^5 for which the NMR study supported a first protonation occurring on such nitrogens (see Fig. 4).

Also in agreement with the spectroscopic results, the molecular orbital calculations show that, in the case of L^3 the HOMO is made up exclusively from the atomic orbitals of the aromatic unit suggesting a more random first protonation. Similar treatment shows for L^6 an important contribution of the atomic orbitals of the central nitrogen atoms to the HOMO, again in good agreement with the protonation pattern found.[21] An analogous situation is observed for L^3 in the highest molecular orbital occupied by an amine lone pair, which is similar to the HOMO of L^3 being also made up preferentially from the atomic orbitals of the central nitrogen atoms.

Cu^{2+} co-ordination

Stability constants. Table 2 shows the logarithms of the stability constants for the formation of Cu^{2+} complexes of thiophenophanes L^1–L^3. By means of comparison, in the same Table 2 are also included the formation constants of the Cu^{2+} complexes of the related paraazacyclophanes L^4–L^6, taken from the literature.[4,7] For molar ratios $[Cu^{2+}]/[L] = 1$ the speciation model of all three receptors is rather similar, and in the

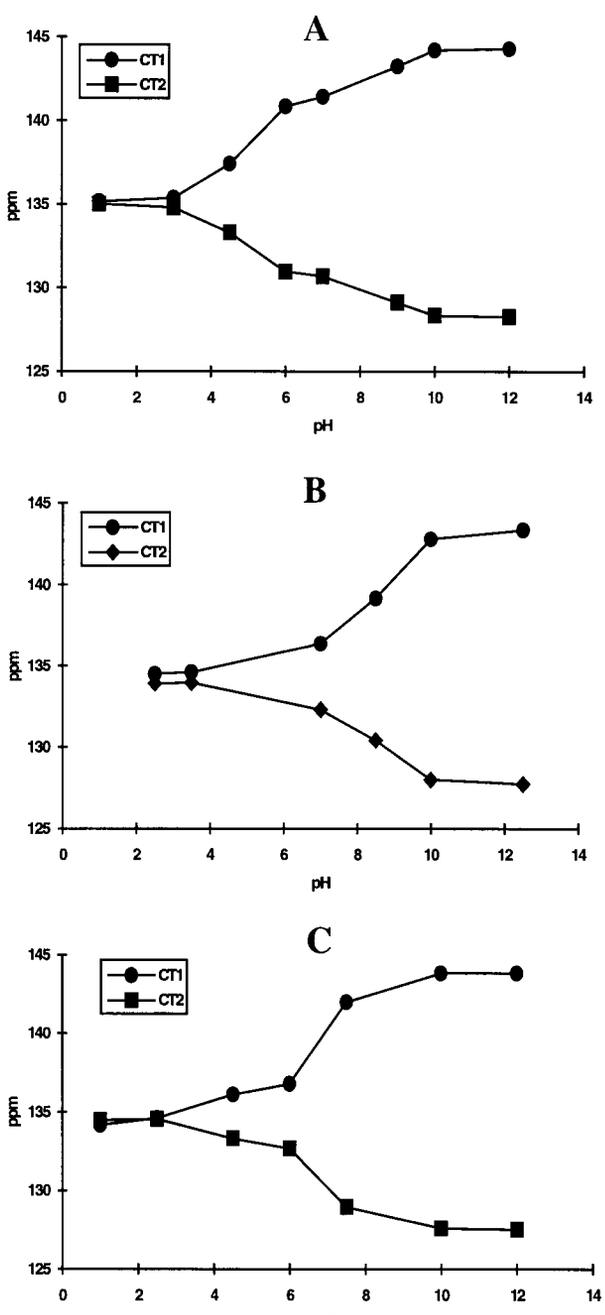

Fig. 2 Plots of the ^{13}C NMR chemical shifts of the aromatic carbon atoms CT1 and CT2 as a function of pH. A) L^1, B) L^2 and C) L^3.

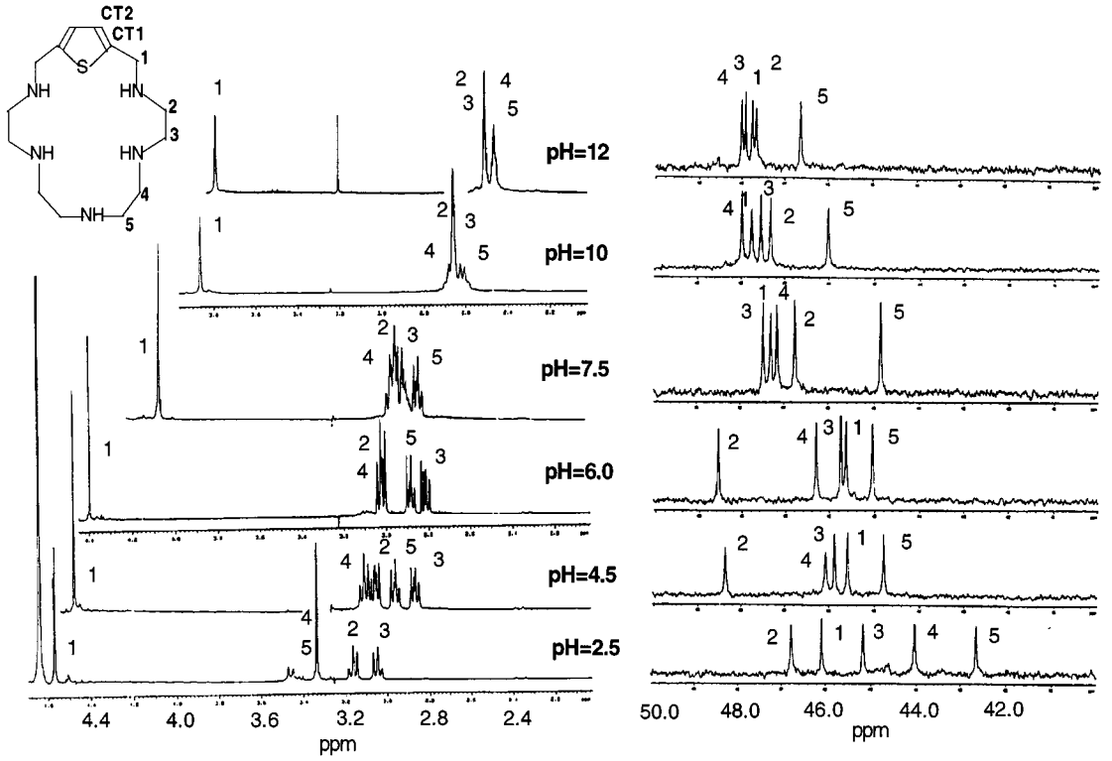

Fig. 3 ^{1}H and ^{13}C NMR spectra of L^3 recorded at different pH values.

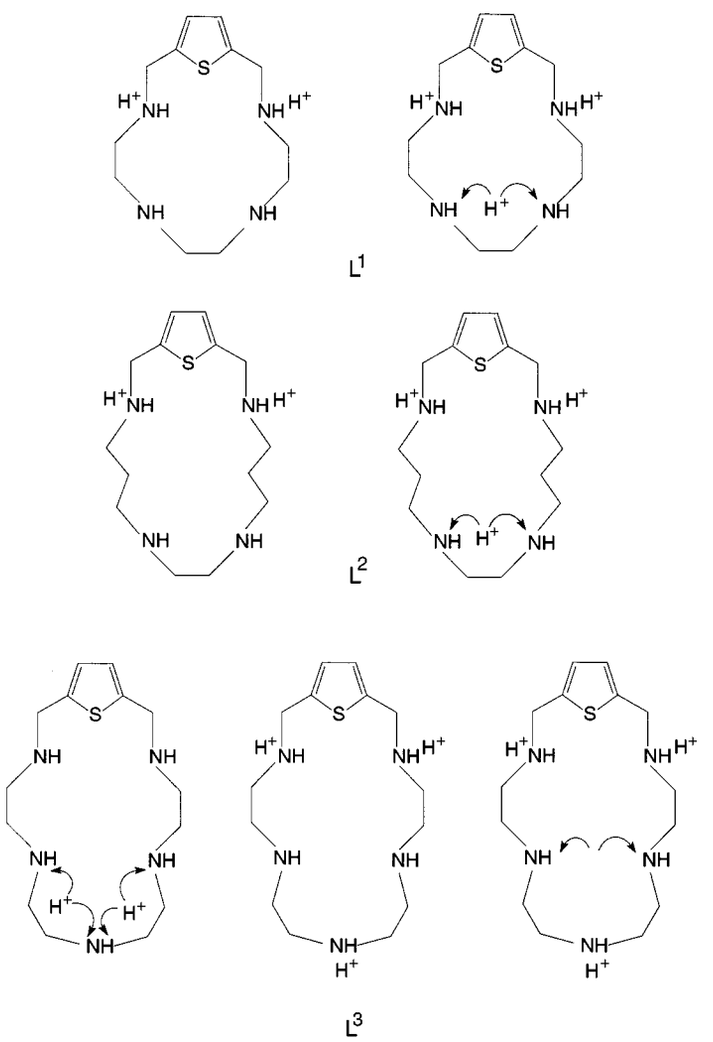

Scheme 2

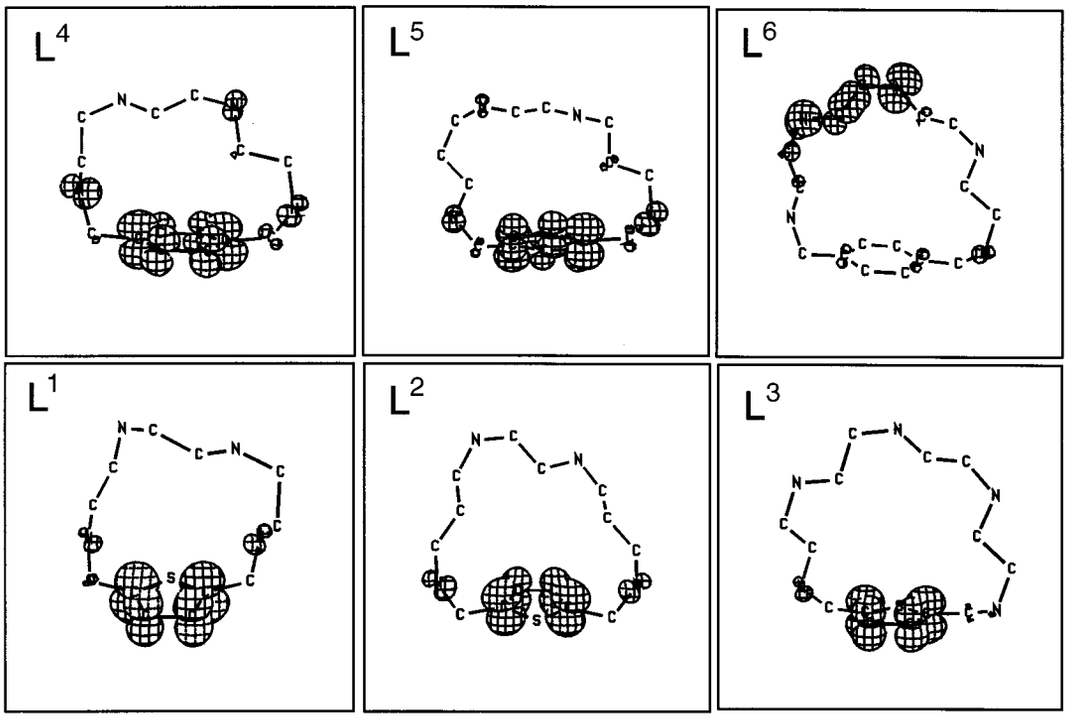

Fig. 4 HOMO orbitals of ligands L^1–L^6.

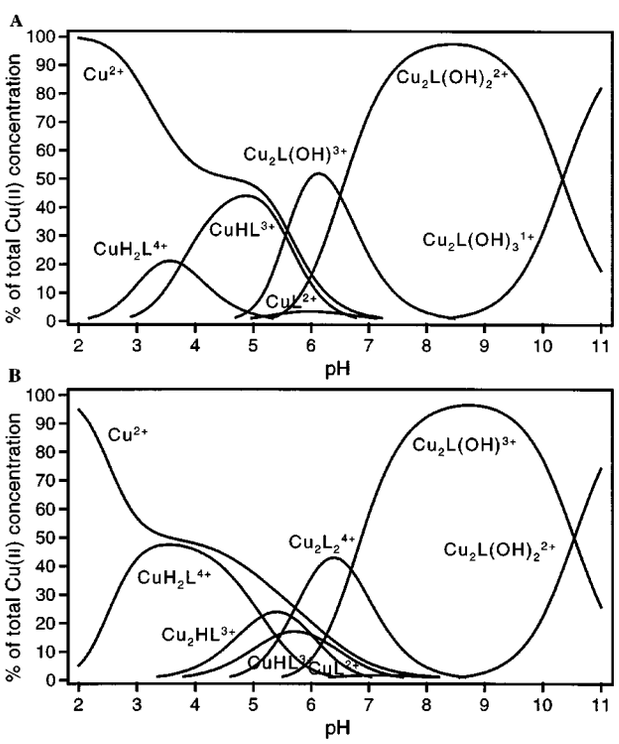

Fig. 5 Distribution diagrams for the systems Cu^{2+}–L^1 (A) and Cu^{2+}–L^3 (B) ($[Cu^{2+}] = 2 \times 10^{-3}$ mol dm^{-3}, $[L] = 10^{-3}$ mol dm^{-3}).

pH range 2.5–10.5 formation of $[CuH_2L]^{2+}$, $[CuHL]^{3+}$ and $[CuL]^{2+}$ species is detected. The only difference among them comes from the fact that while L^1 and L^2 also form a hydroxylated $[CuL(OH)]^+$ species, no such species are detected for L^3, at least in the pH range explored. However the situation is quite different for molar ratios $[Cu^{2+}]/[L] = 2$, since in these conditions binuclear species $[Cu_2L(OH)]^{3+}$, $[Cu_2L(OH)_2]^{2+}$ and $[Cu_2L(OH)_2]^{2+}$ are found for L^1 and $[Cu_2L]^{4+}$, $[Cu_2L(OH)]^{3+}$ and $[Cu_2L(OH)_2]^{2+}$ for L^3. These binuclear species, as shown in the distribution diagram in Fig. 5, are predominant in solution over a wide pH range. Interestingly enough, for L^2 no such species are detected and, in this case, formation of Cu^{2+} hydroxide can be observed above pH 8.

The stability constants of the $[CuL]^{2+}$ species of all three thiophenophanes are rather low in comparison with related tetraaamines or pentaazacycloalkanes either of an open-chain or a cyclic nature being, however, much closer to those reported for triamines.[25] On the other hand, the first protonation constants of the $[CuL]^{2+}$ species (see Table 2) are very large and present comparable or even higher magnitudes than the protonation constants of the corresponding doubly charged cation $[H_2L]^{2+}$ in the free receptors (Table 1), suggesting that protonation of the Cu^{2+} complexes occurs on non-co-ordinated nitrogen atoms. Therefore, all these data support an incomplete involvement of all the nitrogen donors of the receptors in the co-ordination to a single metal ion. The UV-Vis spectra of these systems also give support to this conclusion. For instance, in the system Cu^{2+}–L^2 the visible spectra of the $[CuL]^{2+}$ and $[CuHL]^{3+}$ species are identical ($\lambda = 597$ nm, $\varepsilon = 153$ mol dm^{-3}).

Probably the most noticeable feature in the chemistry of these ligands is the formation of Cu^{2+} binuclear complexes by L^1 and L^3. Interestingly, the receptor L^2 of intermediate size between L^1 and L^3 does not form this kind of complex. This behaviour, which parallels that found for paraazacyclophanes L^4–L^6,[7] can be explained in terms of a balance between flexibility, size and the number of nitrogen atoms of the receptors. The larger the adaptability of the polyamine bridge the better it can fit the coordination requirements of a single metal ion, whereas a large number of nitrogen donors will tend to favour the formation of polynuclear complexes.

The important Cu^{2+} hydroxylated species formed (see Fig. 5) together with the low number of nitrogen donors involved in the first co-ordination sphere of the metals, make these systems potential catalysts for the activation of small molecules. Indeed, many metallobiomolecules with hydrolytic or redox catalytic activity present co-ordination environments displaying similar features.

Electrochemistry. The electrochemical behaviour of the Cu^{2+}–thiophenophane systems is sensitive to the electrode material, solution composition, pH changes and voltammetric parameters. In acidic media no adduct species are formed and

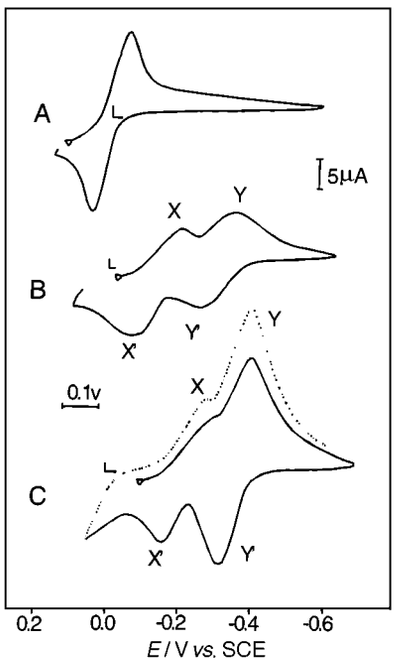

Fig. 6 Cyclic voltammograms at the hanging drop mercury electrode (scan rate, 0.15 V s^{-1}) for $NaClO_4$ 0.15 M solutions of A) $Cu(ClO_4)_2$ 1.07×10^{-3} mol dm^{-3}, pH = 2.35; B) as for A plus L^5 1.12×10^{-3} mol dm^{-3}, pH = 8.60; C) as for A plus L^2 1.22×10^{-3} mol dm^{-3}, pH = 9.95.

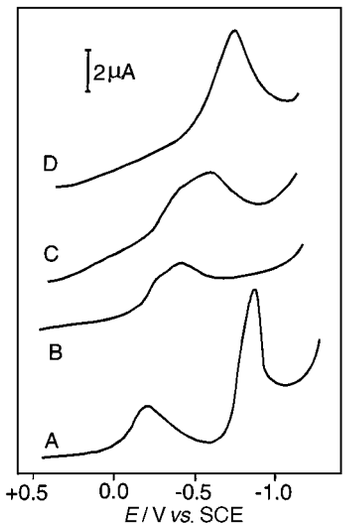

Fig. 7 Cathodic differential pulse voltammograms for the Cu–L^3 system in $NaClO_4$ 0.15 mol dm^{-3}. A) Cu^{2+} 0.40×10^{-3} mol dm^{-3} plus L^3 0.20×10^{-3} mol dm^{-3}, pH 3.4; B) as for A, pH 5.0; C) as for A, pH 10.7; D) Cu^{2+} 0.40×10^{-3} mol dm^{-3} plus L^3 0.45×10^{-3} mol dm^{-3}, pH 11.4. GCE, $v = 20$ mV s^{-1}; pulse width 10 mV.

the CV is identical to that obtained in the absence of the macrocyclic ligand, consisting of a single two-electron reversible couple at the potential expected for the Nernstian Cu^{2+}/Cu(Hg) reduction (Fig. 6A). As demonstrated by cyclic voltammetry at fast scan rates, the electrochemical behaviour, however, is more complicated, involving two successive one-electron steps coupled with dehydration and hydrolysis reactions of the parent Cu^{2+} and the intermediate Cu^{+} species (electrochemical chemical electrochemical (ECE) and disproportionation mechanisms).[26]

As previously reported,[9,10] for neutral and alkaline media solutions containing equimolar amounts of Cu^{2+} and tetraazacyclophanes with benzene or durene spacers two nearly identical couples appear that can be assigned to the electrode processes (eqns. (1) and (2)). This voltammetric pattern is representative of the stabilisation of the Cu^{+} species with respect to its disproportionation into Cu^{2+} and Cu^{0} caused by coordination to macrocyclic receptors (Fig. 6B).

$$Cu^{II}H_pL^{(p+2)} + e^- = Cu^{I}H_pL^{(p+1)} \quad (1)$$

$$Cu^{I}H_pL^{(p+1)} + e^- = Cu^{0} + H_pL^{p+} \quad (2)$$

This behaviour contrasts with that exhibited by the systems consisting of Cu^{2+}–thiophenophane receptors, which is depicted in Fig. 6C. At a mercury electrode, neutral and alkaline solutions containing equimolar amounts of Cu^{2+} and of the thiophenophane receptors display two quasi-reversible overlapped couples (X,X′, Y,Y′) in the potential region between 0.2 and −0.2 V *vs.* SCE. In successive scans, both cathodic peaks are enhanced. This feature is especially relevant for peak Y, denoting that the electrode reaction is mediated by adsorption of the electroactive species on the mercury electrode.[27] These voltammetric data may be adjusted to an ECE mechanism[28] in which a relatively slow reaction is coupled between two successive electron charge transfers assuming that the second transfer occurs at a potential less negative than the first one, resulting in an apparent two-electron couple. Accordingly, the overall electrochemical reactions (3)–(5) can

$$Cu^{II}(H_pL)^{(p+2)}(sol) + e^- = Cu^{I}(H_pL)^{(p+1)}(sol) \quad (3)$$

$$Cu^{I}(H_pL)^{(p+1)}(sol) = Cu^{I}(H_pL)^{(p+1)}(ads) \quad (4)$$

$$Cu^{I}(H_pL)^{(p+1)}(ads) + e^- = Cu^{0}(Hg) + H_pL^{p+} \quad (5)$$

be considered as operative (ECE mechanism). The intermediate step must correspond to an adsorption process that can be accompanied by a rearrangement of the coordination sites.

This scheme is supported by cyclic voltammetry at glassy carbon electrodes. Although at solid electrodes the voltammetric response of Cu^{2+} solutions is complicated by adatom diffusion on the electrode,[29] formation of film oxides,[30,31] *etc.*, significant differences were obtained between macrocyclic ligands containing benzene and thiophene groups.

For L^1 and L^3 dinuclear species are formed in neutral and alkaline media. As can be seen in Fig. 7, differential pulse voltammograms for solutions containing Cu^{2+} and the ligand in a 2:1 stoichiometric ratio exhibit significant variations upon pH changes. Below pH 4, two well-defined peaks at −0.20 and −0.87 V appear, corresponding to successive one-electron reductions of copper (curve A). Upon increasing the pH, the first cathodic peak is followed by a second overlapped peak at −0.45 V (curve B). At alkaline pH values (curve C), two overlapped peaks at −0.45 and −0.60 V appear. This electrochemical response suggests that relatively stable Cu^{+} intermediate species are involved. In solutions containing a 1:1 Cu:L stoichiometric ratio (curve D), only one peak close to −0.65 V is recorded suggesting a chemical electrochemical (CE) mechanism involving the dissociation of the copper–macrocycle adduct preceding a two-electron transfer reaction as described, for instance, for hydroxylate and carbonate adducts.[32]

The cyclic voltammetric pattern previously described denotes the stabilization of Cu^{+} species with disproportionation into Cu^{2+} and Cu^{0} (eqn. (6)). As previously described,[9,10] a direct

$$2\,Cu_m^{I}(H_pL)^{(p+m)} = Cu_m^{II}(H_pL)^{(2m+p)} + mCu^{0} + H_pL^{p+} \quad (6)$$

estimate of the formation constants of $Cu^{I}(H_pL)^{(p+1)}$ species can be made, providing the formation constants of the Cu^{II}-$(H_pL)^{(p+2)}$ species are known, from the relationship (at 298 K) (7); β^{I} and β^{II} refer to the cumulative formation constants of the Cu^{I} and Cu^{II} complexes, respectively.

$$\log \beta^{I} = \log \beta^{II} + m[E^\circ - E^\circ(Cu^{2+}/Cu^{+})]/59 \quad (7)$$

Eqn. (7) holds at selected pH values for which only one

Table 3 Formal potential for the Cu^{2+}/Cu^{+} couple and stability constants (0.15 mol dm^{-3} $NaClO_4$ at 298 K) for the Cu^{2+} and Cu^{+} complexes with polyazamacrocyclic ligands containing aromatic spacers L. Equilibrium constants for the disproportionation process calculated from cyclic voltammetric data

Species	pH	$E^{o\prime}$/mV	log β^{II}	log β^{I}	log K'_d
$[Cu(L^1)]^{2+}$	8.0	−250	11.89	9.1	−0.1
$[CuH(L^1)]^{3+}$	5.5	−220	18.48	16.2	1.6
$[Cu(L^1)(OH)]^{+}$	10.5	−275	3.14	−0.08	−4.2
$[Cu_2(L^1)(OH)_2]^{2+}$	9.0	−255	3.76	−2.0	−2.0
$[Cu(L^2)]^{2+}$	8.0	−180	12.28	10.7	−2.9
$[CuH(L^2)]^{3+}$	7.0	−170	20.16	18.7	−1.2
$[Cu(L^3)]^{2+}$	10.0	−290	14.37	10.9	−1.1
$[CuH(L^3)]^{3+}$	6.5	−220	21.77	19.5	−1.3
$[Cu_2(L^3)(OH)]^{3+}$	9.0	−260	12.54	5.9	−0.6
$[Cu_2(L^3)(OH)_2]^{2+}$	11.5	−280	2.0	−4.6	−3.8
$[Cu(L^5)]^{2+}$ [a]	8.4	−150	13.02(1)	11.9(2)	−4.5(5)
$[CuH(L^5)]^{3+}$ [a]	7.2	−150	20.82(1)	19.7(2)	−2.2(5)
$[Cu(L^{10})]^{2+}$ [a]	8.5	−140	13.35(3)	12.6(2)	−5.6(4)
$[CuH(L^{11})]^{3+}$ [a]	7.0	−140	20.79(1)	19.8(2)	−2.0(4)

[a] Values taken from references 9,10.

adduct species predominates in solution and that is also valid for the hydroxylated complexes. The cumulative formation constants of the Cu^{+} complexes (β^{I}) calculated from cyclic voltammetric data are presented in Table 3 in logarithmic form. An estimate of the equilibrium constant, K'_d for the disproportionation reaction (6) can be obtained through the relationship (8),[9,10] where K_d (log $K_d = 6.24$ at 298 K) represents the

$$\log K'_d = 2\log \beta^{I} - \log \beta^{II} - m\log K_d + \log \beta_p \quad (8)$$

equilibrium constant for the disproportionation of the Cu^{+}(aq) into Cu^{2+}(aq) and Cu^{0}. β_p represents the cumulative protonation constant for the H_pL^{p+} species. For the dismutation of the Cu–L hydroxylated complexes, eqn. (9) holds, and the equation

$$2\ Cu_m^{I}L(OH)_z^{(m-z)} = Cu_m^{II}L(OH)_x^{(2m-x)} + mCu^0 + L + (2z - x)OH^- \quad (9)$$

for K'_d becomes eqn. (10).[9,10] The K'_d values estimated for the equilibrium constants are also summarized in Table 3.

$$\log K'_d = 2\log \beta^{I} - \log \beta^{II} - m\log K_d - (2z - x)\log K_w \quad (10)$$

On comparing the stability constants β^{I} and β^{II} in Table 3 for the different compounds, it can be concluded that substitution of benzene or durene spacers by a thiophene group does not increase the binding strength towards both Cu^{2+} and Cu^{+} oxidation states.

In this respect, it should be noted that contrary to the popular belief that sulfur donors stabilise the Cu^{+} oxidation state, Cu^{+} exhibits little preference between saturated N and S donor atoms.[33] Thus, whereas the stability constants for a series of Cu^{2+} complexes with polyamino polythiaether ligands increase significantly upon increasing the number of sulfur atoms, the stability constants for Cu^{+} complexes remain constant. Accordingly, eventual coordination with an aromatic S atom of low nucleophilic character should not produce any particular enhancement in the binding affinity of the metal ion.

The cyclic voltammetric data suggest that two different coordinative arrangements of metallic centre are possible for thiophene ligands. For Cu^{2+} adducts, the coordination takes place mainly *via* nitrogen atoms as described for ligands containing benzene and durene spacers and the electrochemical reduction occurs in two reversible one-electron steps. Although, as previously discussed, adsorption-mediated electrochemical processes are involved for ligands containing thiophene spacers, a possible weak co-ordination of the reduced Cu^{+} by the sulfur atom could also contribute to the observed change in the mechanism.

We are currently extending these studies to unravel the electrochemical reduction mechanism and to test the possible use of these complexes as catalysts assisting a variety of processes.

Acknowledgements

We thank DGICYT Project No. PB96-0792-CO2 and Generalitat Valenciana Project No. GV-D-CN-09-140–16 for financial support.

References

1 A. Bencini, M. I. Burguete, E. García-España, S. V. Luis, J. F. Miravet and C. Soriano, *J. Org. Chem.*, 1993, **58**, 4749.
2 M. I. Burguete, B. Escuder, E. García-España, S. V. Luis and J. F. Miravet, *J. Org. Chem.*, 1994, **59**, 1067.
3 M. I. Burguete, B. Escuder, E. García-España, S. V. Luis and J. F. Miravet, *Tetrahedron Lett.*, 1994, 9075.
4 A. Andrés, M. I. Burguete, E. García-España, S. V. Luis, J. F. Miravet and C. Soriano, *J. Chem. Soc., Perkin Trans. 2*, 1993, 749.
5 M. A. Bernardo, J. A. Parola, F. Pina, E. García-España, V. Marcelino, S. V. Luis and J. F. Miravet, *J. Chem. Soc., Dalton Trans.*, 1995, 993.
6 E. García-España and S. V. Luis, *Supramol. Chem.*, 1996, **6**, 257.
7 A. Andrés, C. Bazzicalupi, A. Bianchi, E. García-España, S. V. Luis, J. F. Miravet and J. A. Ramírez, *J. Chem. Soc., Dalton Trans.*, 1994, 1995.
8 B. Escuder, E. García-España, J. Latorre, S. V. Luis and J. A. Ramírez, in preparation.
9 A. Doménech, J. V. Folgado, E. García-España, S. V. Luís, J. M. Llinares, J. F. Miravet and J. A. Ramírez, *J. Chem. Soc., Dalton Trans.*, 1995, 541.
10 A. Doménech, E. García-España, V. Marcelino, B. Altava, S. V. Luís, J. F. Miravet, A. Bianchi and L. Ferrini, *Inorg. Chim. Acta*, 1996, **252**, 123.
11 E. Garcia-España, M. J. Ballester, F. LLoret, J. M. Moratal, J. Faus and A. Bianchi, *J. Chem. Soc., Dalton Trans.*, 1988, 101.
12 M. Fontanelli and M. Micheloni, *Proceedings of the I Spanish-Italian Congress on Thermodynamics of Metal Complexes*, Peñíscola, Spain, 1990. Program for the automatic control of the burette additions and electromotive force readings.
13 G. Gran, *Analyst* (*London*), 1952, **77**, 661; F. J. Rossoti and H. Rossoti, *J. Chem. Educ.*, 1965, **42**, 375.
14 P. Gans, A. Sabatini and A. Vacca, *J. Chem. Soc., Dalton Trans.*, 1985, 1195.
15 A. Vacca, University of Florence, unpublished work, a FORTRAN Program to determine the distribution of the species in multiequilibria systems from the stability constants and mass balance equations.

16 A. K. Convington, M. Paabo, R. A. Robinson and R. G. Bates, *Anal. Chem.*, 1968, **40**, 700.
17 C. Mealli and D. Proserpio, *J. Chem. Educ.*, 1990, **67**, 399.
18 HYPERCHEM 3.0 from Hypercube, Inc., Waterloo, ON, Canada. VRL. http://www.hyper.com.
19 J. E. Richman and T. J. Atkins, *J. Am. Chem. Soc.*, 1974, **96**, 2268; J. E. Richman, T. J. Atkins and W. F. Oetle, *Organic Synthesis*, Wiley, New York, Collect. Vol. VI., p. 652.
20 F. Chavez and D. Sherry, *J. Org. Chem.*, 1989, **54**, 2990; B. K. Vriesema, J. Buter and R. M. Kellog, *J. Org. Chem.*, 1994, **49**, 110; D. M. Trost, H. C. Arndt, P. E. Strege and T. R. Verhoeven, *Tetrahedron Lett.*, 1976, 3477.
21 A. Bianchi, B. Escuder, E. García-España, S. V. Luis, V. Marcelino, J. F. Miravet and J. A. Ramírez, *J. Chem. Soc.*, *Perkin Trans. 2*, 1994, 1253.
22 M. A. Bernardo, J. A. Guerrero, E. García-España, S. V. Luis, J. M. Llinares, F. Pina, S. V. Luis, J. A. Ramírez and C. Soriano, *J. Chem. Soc.*, *Perkin Trans. 2*, 1996, 2335.
23 J. E. Sarnesky, H. L. Surprenant, F. K. Molen and C. N. Reileg, *Anal. Chem.*, 1975, **47**, 2116.
24 D. N. Hague and A. D. Moreton, *J. Chem. Soc.*, *Perkin Trans. 2*, 1994, 265.
25 A. E. Martell, R. M. Smith and R. M. Moteikaitis, NIST Critical Stability Constants Database; Texas A&M, University College Station, TX, 1993.
26 (*a*) M. Mastragostino, L. Nadjo and J. M. Saveant, *Electrochim. Acta*, 1968, **13**, 721; (*b*) M. Mastragostino and J. M. Saveant, *Electrochim. Acta*, 1968, **13**, 751; (*c*) F. M. Hawkridge and H. H. Bauer, *Anal. Chem.*, 1972, **44**, 364; (*d*) J. L. Anderson and I. Shain, *Anal. Chem.*, 1976, **48**, 1274; (*e*) J. L. Anderson and I. Shain, *Anal. Chem.*, 1978, **50**, 163.
27 A. J. Bard and L. R. Faulkner, *Electrochemical Methods*, Wiley & Sons, New York, 1980.
28 R. S. Nicholson and I. Shain, *Anal. Chem.*, 1965, **37**, 178.
29 L. H. Jenkins, *J. Electrochem. Soc.*, 1970, **117**, 630.
30 J. J. Kruger, *J. Electrochem. Soc.*, 1959, **106**, 847.
31 G. T. Miller and K. R. Lawless, *J. Electrochem. Soc.*, 1959, **106**, 854.
32 M. S. Shuman and L. C. Michael, *Anal. Chem.*, 1978, **50**, 2104.
33 M. M. Bernardo, M. J. Heeg, R. R. Schroeder, L. A. Ochrymowycz and D. A. Rorabacher, *Inorg. Chem.*, 1992, **31**, 191.

Paper 9/00700H